

## Analysis of key comfort properties of rib-knitted fabrics in relation to fabric structure

Azita Asayesh<sup>a</sup> & Zahra Ghanbari

Department of Textile Engineering, Amirkabir University of Technology, Tehran 15875 4413, Iran

Received 21 September 2024; revised received and accepted 4 February 2025

This study aims to examine the effect of float stitches on the key comfort properties of rib-knitted fabrics. Knit pattern, as a structural parameter, plays a significant role in determining fabric behaviour, and this research evaluates how variations in float stitches affect air permeability, water vapour permeability, thermal resistance, and related comfort characteristics. The findings show that incorporating float stitches reduces both air and water vapour permeability, while increasing thermal resistance, thereby making these fabrics more suitable for winter clothing due to enhanced thermal insulation. An increase in the number of float stitches across successive courses further raises water vapour permeability, thermal resistance, and energy absorption, but lowers air permeability and resiliency. When float stitches are present on both sides of the fabric, thermal resistance, energy absorption, resiliency, and thickness recovery improve, whereas air permeability, water vapour permeability, and relative compressibility decrease compared to fabrics with floats on only one side. The study indicates that fabrics with float stitches on one side are better suited for summer clothing due to their improved moisture management, while those with float stitches on both sides are more suitable for winter use, owing to their superior thermal insulation.

**Keywords:** Comfort, Fabric structure, Float stitch, Weft-knitted fabric

### 1 Introduction

Comfort is one of the most important performance attributes of a textile material, arising from a state of mental and physical equilibrium between the human body and its surrounding environment<sup>1</sup>. It is generally categorised into psychological, thermo-physiological, tactile, and physical comfort<sup>2</sup>. Psychological comfort relates to sensory perception and fashion preferences; thermo-physiological comfort concerns the transmission of heat, air, and moisture through the fabric; tactile comfort depends on surface characteristics and mechanical behaviour; and physical comfort is associated with garment fit and ease of movement.

A wide range of factors influences clothing comfort, including fibre type<sup>3-5</sup>, yarn parameters such as count and spinning system<sup>6-8</sup>, fabric characteristics like thickness, tightness factor, and weight<sup>9-11</sup>, as well as environmental conditions and the wearer's activity level. Extensive research has examined the comfort behaviour of weft-knitted fabrics owing to their widespread use in apparel.

Chidambaram *et al.*<sup>12</sup> reported that increasing the proportion of bamboo fibre enhances the air and water

vapour permeability of cotton/bamboo knitted fabrics, while reducing thermal conductivity. Similarly, Oglakcioglu *et al.*<sup>13</sup> found that higher Angora rabbit fibre content in Angora/cotton knitted fabrics decreases thermal conduction, thermal absorption, and water vapour permeability, but increases fabric thermal resistance. Differences in yarn structure have also been shown to influence comfort behaviour. Jhanji *et al.*<sup>14</sup> examined the effect of fibre type and yarn linear density on plated single-jersey knitted fabrics. Using nylon in the next-to-skin layer resulted in the highest air and water vapour permeability and the coolest initial feel, attributable to its high thermal absorptivity.

Ozdil *et al.*<sup>15</sup> investigated yarn characteristics in rib-knitted fabrics, while Yazdi *et al.*<sup>16</sup> explored heat and moisture transport in double-surface weft-knitted fabrics produced from hydrophilic (cotton) and hydrophobic (polyester, polypropylene) fibres. They concluded that fabrics with a hydrophobic inner layer and a hydrophilic outer layer offer optimal thermal and moisture comfort in hot conditions, as moisture is efficiently transported away from the skin and evaporated through the outer layer. Long<sup>17</sup> similarly reported that water vapour permeability depends on fabric porosity, whereas liquid moisture transfer is

<sup>a</sup>Corresponding author.  
E-mail: a\_asayesh@aut.ac.ir

governed by fibre absorption characteristics and their contrast between layers.

Toma *et al.*<sup>18</sup> observed that the thermophysiological comfort of knitted fabrics is strongly governed by structural parameters such as thickness and mass per unit area. Sayed *et al.*<sup>19</sup> investigated the thermal comfort characteristics of various bi-layer knitted fabrics constructed using Modal/Bamboo yarn for the outer layer and microfibre polyester, polyester, or acrylic yarn for the inner layer. Hossain and Islam<sup>20</sup> showed that vortex-spun neppy yarn fabrics offer notable advantages in moisture management, breathability, and tactile comfort compared to ring-spun counterparts.

Research by Tabassum *et al.*<sup>21</sup> revealed that BCI (Better Cotton Initiative) cotton fabrics exhibit superior thermal comfort as compared to conventional cotton fabrics due to higher air permeability, thermal transmittance, and fibre uniformity, making them ideal for sportswear and summer apparel. In line with the global Green Course strategy, Padleckiene *et al.*<sup>22</sup> produced four new biodegradable three-layer weft-knitted fabrics using sustainable hemp and polylactide fibres. The developed fabrics demonstrated excellent thermal comfort and moisture management properties. Dogan and Kilinc<sup>23</sup> showed that knitting type, tightness, and plied yarn significantly influenced the thermal comfort of 100% cashmere fabrics.

Limeneh *et al.*<sup>24</sup> demonstrated that the comfort performance of knitted fabrics is strongly influenced by their mechanical and surface properties, which vary significantly with fibre composition and structural design. Bivainyte and Mikucioniene<sup>25</sup> studied the influence of structure, fibre type, and yarn properties on the air and water vapour permeability of double-layer knitted fabrics. They noted that, for fabrics with identical patterns, air permeability is primarily determined by loop length, while for fabrics with differing patterns, it can be predicted using the area linear filling rate.

From a structural perspective, Oglakcioglu and Marmarali<sup>1</sup> showed that single-jersey fabrics have lower thermal resistance and higher water vapour permeability compared to rib and interlock structures. Interlock fabrics display the highest thermal resistance and the lowest water vapour permeability, making double-jersey structures more suitable for winter wear, whereas single-jersey fabrics are preferable for summer garments due to their superior moisture management. In subsequent work, the same authors<sup>26</sup> evaluated the effect of moisture on thermal

comfort, demonstrating that wetted fabrics exhibit a cooler handle due to increased thermal absorption and reduced thermal insulation.

Rib is one of the fundamental weft-knitted structures, from which numerous derivatives can be formed using combinations of knit, tuck, and float stitches. These modifications may be introduced for aesthetic reasons or to enhance dimensional and physical performance. The knit pattern represents a key structural variable that significantly affects the mechanical and comfort behaviour of a fabric.

Against this background, the present study aims to investigate the influence of float stitches on the comfort properties of rib weft-knitted fabrics, with the goal of understanding how structural variation affects thermo-physiological performance.

## 2 Materials and Methods

### 2.1 Fabrication of the Samples

Rib-knitted fabrics with varying knit patterns were produced to study the influence of float stitches on comfort-related properties. Fabrics were knitted using 30/3 metric cotton yarn on a 7-gauge STOLL CMS T330 computerised flat knitting machine, under constant knitting conditions (cam setting, yarn input tension, and fabric take-down). The structures differed in the number of float stitches inserted in successive courses. After knitting, all samples were relaxed on a flat surface for 48 hours under standard atmospheric conditions (20 °C, 65 % RH). The knit patterns and corresponding fabric images are presented in Table 1. In the fabric codes, the numeral represents the number of float stitches in the knit repeat. The first, penultimate, and final structures correspond to Rib (R), Half Milano (HM), and Full Milano (FM), respectively.

### 2.2 Structural Evaluation

#### 2.2.1 Density

Due to the structural complexity of the knitted samples, the number of unit cells per unit length ( $C_uPC$ ) and per unit width ( $W_uPC$ ) was determined. These values were multiplied by the number of courses and wales in the knit repeat (Table 1) to obtain the courses per centimetre (c.p.c), and wales per centimetre (w.p.c) using the Eqs. 1 and 2:

$$c.p.c = \frac{\text{Total number of courses}}{\text{Fabric length}} = C_uPC \times \text{Number of courses in the knit repeat} \dots (1)$$

Table 1 — Knit patterns and corresponding images of the fabrics

Fabric code	R	R1	R2	R3	R4	HM	FM
Knit repeat							
Front view							
Back view							

$$w.p.c = \frac{\text{Total number of wales}}{\text{Fabric width}} = W_uPC \times \text{Number of wales in the knit repeat} \quad \dots (2)$$

Measurements were taken at five positions on 7.5 × 7.5 cm<sup>2</sup> samples, and the mean values are reported (Table 2).

**2.2.2 Mass Per Unit Area**

Areal density or mass per unit area was determined according to ASTM D 3776 standard<sup>27</sup>. Four specimens (10 × 10 cm<sup>2</sup>) from each fabric type were conditioned and weighed. Areal density was calculated by dividing the sample's weight by its area. Average values are given in Table 2.

**2.2.3 Thickness**

Fabric thickness was measured using a Shirley digital thickness tester following ASTM D 1777-96 standard<sup>28</sup>. Ten measurements were taken at different points under a pressure of 20 g/cm<sup>2</sup>, and the mean values are reported in Table 2.

**2.2.4 Structural Index**

A structural index was formulated to quantify the proportion of float stitches in each structure as follows:

$$\text{Structural index} = \frac{\text{Number of float stitches in the knit repeat of the fabric}}{\text{Total number of stitches in the knit repeat of the fabric}} \quad \dots (3)$$

The structural index for each fabric is listed in Table 2. As expected, the index increases with higher numbers of float stitches.

**2.3 Comfort Evaluation**

**2.3.1 Air Permeability**

Air permeability was measured using a Shirley SDL air permeability tester, according to the ASTM D73729 standard, with a pressure difference of 25 Pa. Ten specimens per fabric type were tested, and mean values were recorded.

**2.3.2 Water Vapour Permeability**

Water vapour permeability was measured using the cup method according to BS 7209<sup>30</sup> under standard conditions (20 ± 2 °C, 65 ± 5% RH). Four specimens from each fabric were tested, and the average value was recorded. By measuring the weight of the samples before and after the test (5 h), the water vapour permeability was calculated using Eq. 4:

$$\text{Water vapour permeability (kgm}^{-2}\text{h}^{-1}) = \frac{M}{At} \quad \dots (4)$$

where  $M$  is the loss in mass (kg);  $t$ , test duration (h); and  $A$ , internal area of the cup ( $\text{m}^2$ ).

### 2.3.3 Thermal Conductivity

Thermal resistance was measured using the two-plate method in accordance with BS-4745<sup>31</sup> standard. Three specimens per fabric structure were tested, and mean thermal resistance values ( $\text{m}^2 \text{ }^\circ\text{C K/W}$ ) were calculated.

### 2.3.4 Compressibility

Compressional behaviour was assessed using a Shirley digital thickness tester by recording thickness at pressures of 20, 50, 100, 200, 500, 1000, 1500, and 2000  $\text{g/cm}^2$ . The first reading was taken after 30 s at 20  $\text{g/cm}^2$ . The pressure increased successively, and the corresponding thickness was registered. The first recovery recording was performed by releasing the pressure of 2000  $\text{g/cm}^2$  and allowing the fabric sample to recover for 30 s. The succeeding recovery readings were taken using the same method. Ten tests were performed for each fabric, and average compression and recovery curves were generated.

### 2.4 Statistical Analysis

The effect of fabric structure on comfort-related properties was analysed using one-way analysis of variance (ANOVA) at a 95% confidence level, followed by Duncan's post-hoc test. Statistical significance was accepted at  $p < 0.05$ . All analyses were conducted using SPSS software.

## 3 Results and Discussion

### 3.1 Structural Parameters

The structural characteristics of the fabrics are summarised in Table 2. As is evident, an increase in the number of float stitches within the fabric structure results in higher stitch density, which subsequently elevates both the fabric thickness and mass per unit area. This rise in stitch density is primarily linked to the effect of float stitches on loop geometry. As depicted in Figure 1, float loops hold the yarn under

higher tension, drawing yarn from neighbouring knitted loops and reducing loop size<sup>32</sup>. This reduction in loop size increases the course density of the fabric, ultimately contributing to greater fabric thickness and weight.

### 3.2 Air Permeability

Figure 2 demonstrates the air permeability of the fabrics. The Rib fabric (R) exhibits the highest air permeability, with a progressive decrease observed as the structural index increases from R1 to R4. This behaviour is attributed to the influence of float stitches on loop geometry. As mentioned previously, float loops hold the yarn under higher tension, drawing yarn from neighbouring knitted loops and reducing loop size<sup>32</sup>. Consequently, the course density of the fabric increases (Table 2), which in turn reduces the fabric's porosity and subsequently its air permeability.

The same principle explains the lower air permeability of the Half Milano (HM) and Full Milano (FM) structures compared with the Rib. Furthermore, FM shows lower permeability than HM. In the FM, float stitches exist on both sides of the fabric, whereas in HM, float stitches are available on only one side of the fabric. Consequently, the number of float stitches in FM is higher than in HM, which in

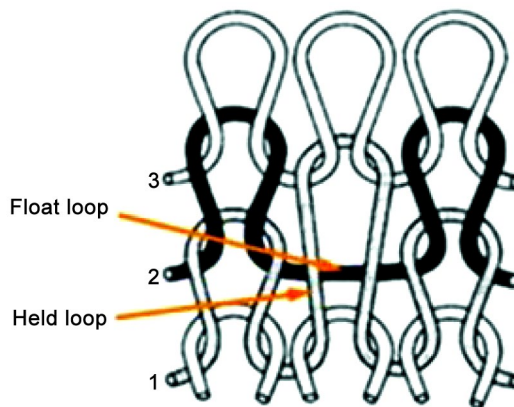


Fig. 1 — Schematic representation of the float stitch in a single jersey knitted fabric

Table 2 — Structural properties of the fabrics

Fabric code	C <sub>u</sub> PC	C.P.C	W <sub>u</sub> PC	W.P.C	Mass per unit area, $\text{g/cm}^2$	Thickness, mm	Structural index
R	5.9	5.9	2.1	4.2	0.047	2.54	0
R1	3.7	7.4	2.3	4.6	0.054	2.73	0.13
R2	2.8	8.4	2.3	4.6	0.057	2.76	0.17
R3	2.2	8.8	2.3	4.6	0.059	2.78	0.19
R4	2	10	2.3	4.6	0.061	2.89	0.20
HM	5.5	11	3.9	3.9	0.055	2.56	0.25
FM	5.3	10.6	3.9	3.9	0.065	2.81	0.33

turn leads to a higher structural index and a subsequently tighter structure. Statistical analysis confirms that the fabric structure significantly affects air permeability ( $P = 0.001$ ).

**3.3 Water Vapour Permeability**

Water vapour is transmitted through fabrics by two mechanisms: passage through open pores and sorption–diffusion through the fibre–yarn matrix, followed by evaporation from the surface<sup>33-34</sup>. Figure 3 illustrates the water vapour permeability results. The rib fabric exhibits the highest water vapour permeability because of its higher porosity, as explained previously. Although the introduction of float stitches from R1 to R4 increases fabric density and reduces porosity, these samples show an increase in water vapor permeability. This suggests that vapour transport predominantly occurs through the second mechanism, namely, adsorption by the fabric's structure and surface evaporation. Furthermore, FM demonstrates lower water vapor permeability than HM, due to its denser structure and lower porosity. Statistical analysis indicates a significant effect of

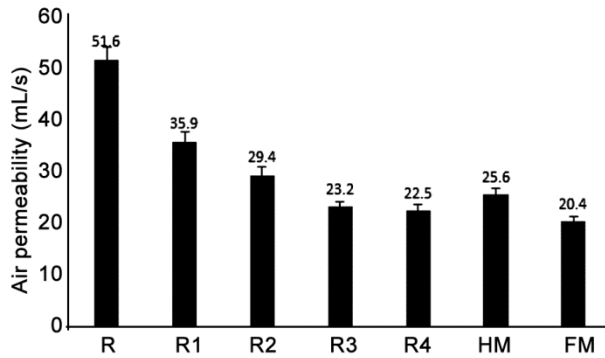


Fig. 2 — Effect of fabric structure on the air permeability of the fabrics

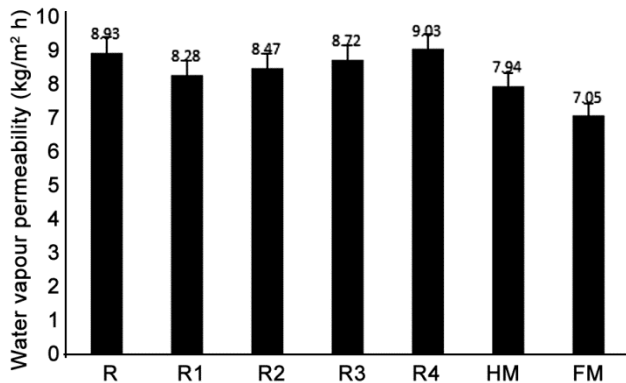


Fig. 3 — Effect of fabric structure on the water vapour permeability of the fabrics

fabric structure on water vapour permeability ( $P=0.013$ ).

**3.4 Thermal Resistance**

Figure 4 shows the thermal resistance values of the fabrics. A clear increasing trend is observed from R1 to R4, with all exhibiting higher resistance than the rib fabric. The presence of float stitches increases both fabric density and thickness (Table 2), resulting in greater entrapped air and, consequently, enhanced thermal resistance.

Between the Milano structures, FM displays higher thermal resistance than HM due to its greater thickness. Statistical results confirm that fabric structure significantly influences thermal resistance ( $P = 0.003$ ).

**3.5 Compressional Properties**

Compressional behaviour was evaluated through compression and recovery curves and quantified using parameters defined by Kawabata<sup>35</sup>. To evaluate the compressional properties, parameters such as the work of compression (WC), work of recovery from compression (W'C), dissipated compression energy ( $E_m$ ), resilience (RC), relative compressibility (EMC), thickness change ( $\Delta T$ ), and thickness recovery (TR) have been calculated as follows:

$$WC = \int_{T_{Oc}}^{T_m} P_c dV = \int_{T_{Oc}}^{T_m} P_c dt_c \quad \dots (5)$$

$$W'C = \int_{T_m}^{T_{Or}} P_r dV = \int_{T_m}^{T_{Or}} P_r dt_r \quad \dots (6)$$

$$E_m = WC - W'C \quad \dots (7)$$

$$RC = \frac{W'C}{WC} \times 100 \quad \dots (8)$$

$$EMC = (1 - \frac{T_m}{T_{Oc}}) \times 100 \quad \dots (9)$$

$$\Delta T = T_{Oc} - T_m \quad \dots (10)$$

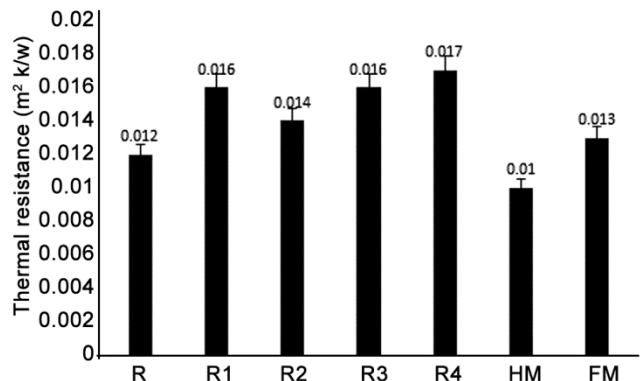


Fig. 4 — Effect of fabric structure on the thermal resistance of the fabrics

Table 3 — Compression parameters of the spacer fabrics

Fabric code	WC, cN.mm/cm <sup>2</sup>	W'C, cN.mm/cm <sup>2</sup>	E <sub>m</sub> , cN.mm/cm <sup>2</sup>	RC, %	ΔT, mm	TR, %
R	540.9	370.9	170	68.6	1.63	74.7
R1	739.8	338.4	401.4	45.7	1.59	76.9
R2	751.5	329.8	421.7	43.9	1.65	75.7
R3	768.5	270.9	497.6	35.3	1.64	75.9
R4	773.7	245.3	528.4	31.7	1.73	72.2
HM	727.6	249.3	478.3	34.3	1.5	76.8
FM	812.8	299.1	513.7	36.8	1.5	82.6

$$TR = \frac{T_{or}}{T_{oc}} \times 100 \quad \dots (11)$$

where suffixes c and r represent the compression and recovery state, respectively; P, pressure; T, fabric thickness; T<sub>oc</sub>, initial thickness of the fabric under the pressure of 20 g/cm<sup>2</sup>; T<sub>m</sub>, thickness of the fabric under the pressure of 2000 g/cm<sup>2</sup>; and T<sub>or</sub>, thickness of the fabric at the end of the compression recovery cycle. Table 3 lists the mean values for these parameters.

### 3.5.1. Energy Absorption

The effect of fabric structure on the absorbed energy (WC) by the fabric is illustrated in Fig. 5(a). It shows that the Rib fabric absorbs the least compression energy. WC increases steadily from R1 to R4 as the structural index increases. The reason is that the higher proportion of float stitches produces a tighter structure, which resists compression more effectively and therefore requires greater energy for compression.

Due to the same reason, the Milano structures exhibit higher energy absorption than Rib, with FM showing the maximum due to the float stitches present on both sides. Statistical analysis confirms a significant influence of fabric structure on WC ( $P=0.000$ ).

### 3.5.2 Dissipated Compression Energy

Dissipated compression energy (E<sub>m</sub>) represents the difference between the work of compression (WC) and the work of recovery from compression (W'C). Fig. 5(b) demonstrates that the E<sub>m</sub> follows the same trend as WC: Rib shows the lowest dissipation, while values increase progressively from R1 to R4. FM exhibits the highest dissipation, followed by HM, due to their tighter structures. As Table 3 indicates, WC increases while W'C decreases with a higher structural index, producing a significant rise in E<sub>m</sub> ( $P=0.000$ ).

### 3.5.3 Resilience

The ability of a material to return to its original form and shape after deformation is called resilience (RC). RC results are presented in Fig. 5(c). Rib fabric shows the highest resilience, whereas RC decreases consistently from R1 to R4. This is explained by the decreasing W'C and increasing WC as the number of float stitches increases, thereby reducing the W'C/WC ratio. FM demonstrates higher resilience than HM, but both remain lower than Rib. This effect is statistically significant ( $P=0.000$ ).

### 3.5.4 Relative Compressibility

Figure 5(d) displays the relative compressibility of the fabrics. As seen, the relative compressibility of the Rib fabric is the highest among the considered fabrics. This can be attributed to the fact that the presence of float stitches in the fabric structure increases the fabric's tightness, and ultimately, the fabric resists compression more effectively. FM shows lower compressibility than HM because floats occur on both sides. The overall effect of structure on compressibility is statistically significant ( $P=0.000$ ).

### 3.5.5 Thickness Change and Recovery

Thickness change (ΔT), shown in Figure 5(e), does not differ significantly between Rib and samples R1–R3. However, both Milano fabrics exhibit a smaller ΔT than Rib, owing to their denser structures, which offer greater resistance to compression.

Thickness recovery represents the percentage of the fabric's thickness that recovers after the compressional force is eliminated. Figure 5(f) shows the thickness recovery results. It indicates that the Rib fabric has lower thickness recovery than other fabric structures. As mentioned previously, fabrics containing float stitches in their structure resist more compression and exhibit less thickness change. Hence, after the load is removed, their thickness is closer to their initial thickness. In other words, their thickness recovery is higher than that of the Rib

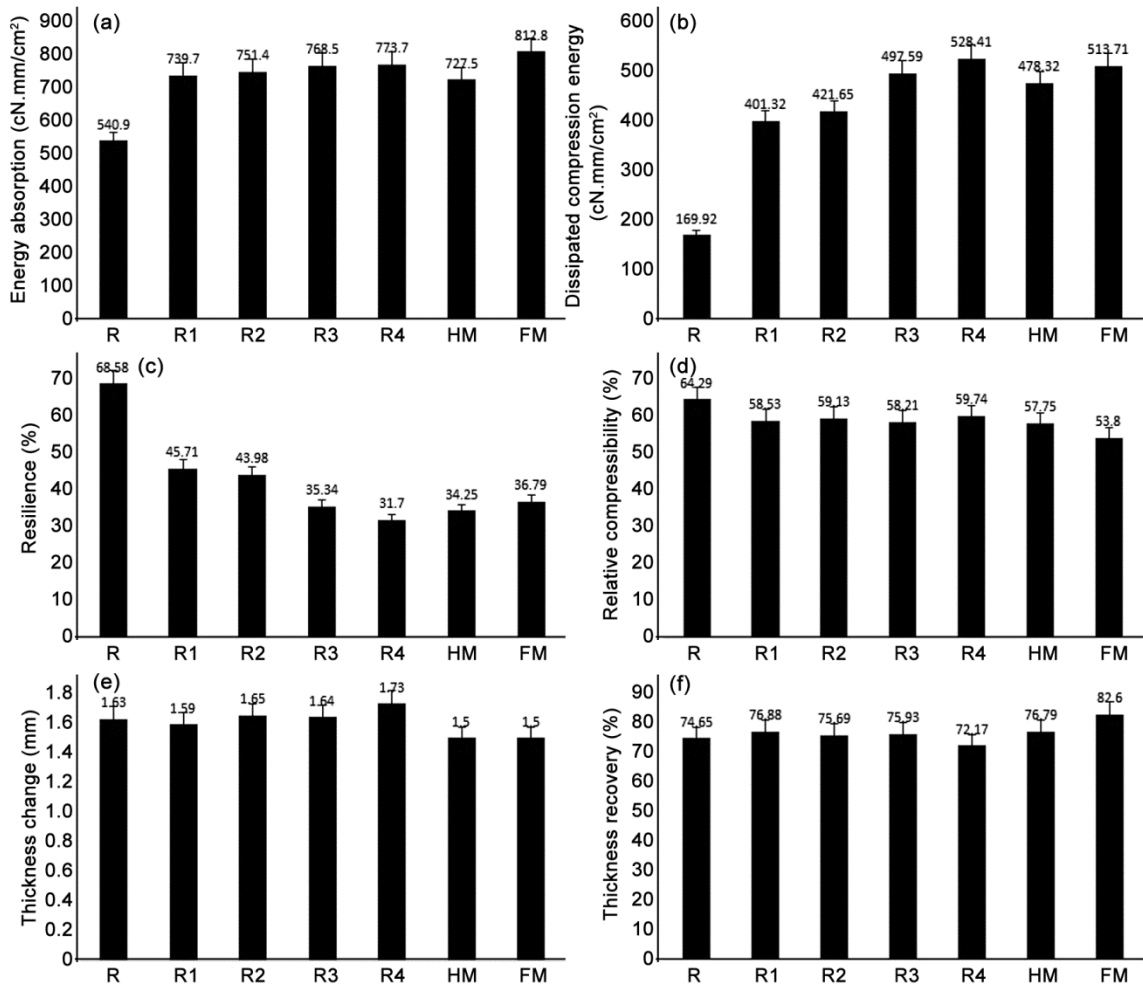


Fig. 5 — Effect of fabric structure on the compressional characteristics (a) energy absorption, (b) dissipated compression energy, (c) resilience, (d) relative compressibility, (e) thickness change, and (f) thickness recovery

fabric. Between Milano structures, FM shows higher TR than HM due to the greater number of float stitches. No significant differences are observed among R1–R3, while R4 exhibits slightly lower TR, likely due to its higher initial thickness.

**4 Conclusion**

The results of this study confirm that fabric structure plays a decisive role in governing the air permeability, water vapour permeability, thermal resistance, and compressional behaviour of knitted fabrics. Rib fabric consistently exhibits the highest air and water vapour permeability owing to its greater porosity. As the structural index increases from R1 to R4, the presence of float stitches tightens the structure, reduces porosity, and subsequently decreases air permeability, while enhancing thermal resistance. FM, characterised by float stitches on both

sides, demonstrates lower air and water vapour permeability and higher thermal resistance compared with HM due to its denser configuration. The compressional analysis reveals that fabrics with higher structural indices absorb more energy and dissipate more compression energy yet show lower resilience and lower relative compressibility. The reduced thickness change and improved thickness recovery of float-stitch fabrics further indicate their superior resistance to compression. In terms of thermo-physiological comfort, fabrics containing float stitches are more suitable for winter clothing because their higher density and thickness provide greater thermal insulation. FM is the most appropriate for cold weather use due to its superior thermal resistance, while HM is preferable for summer garments as it offers better air and water vapour permeability.

### Acknowledgement

The authors gratefully acknowledge the financial support provided by the Amirkabir University of Technology (Grant number: 40/1119).

### References

- 1 Oglakcioglu N A & Marmarali, *Fibres Text East Eur*, 15 (5) (2007) 64.
- 2 Gokarneshan N, *Juniper Online J Mater Sci*, 5 (3) (2019) 1.
- 3 Abbasi S A, Marmarali A & Ertekin G, *Int J Cloth Sci*, 32 (6) (2020) 837.
- 4 Mohapatra S, Vidya T, Kumar D V, Rajwin A J, Babu V R, Prakash C, Shah B A & Roy R, *Fibres Text East Eur*, 29 (5) (2021) 50.
- 5 Santhanam S & Selvaraj S K, *J Text Appar Technol*, 12 (3) (2022) 1.
- 6 Coruh E, *Fibres Text East Eur*, 23 (4) (2015) 66.
- 7 Vadicherla T & Saravanan D, *Indian J Fibre Text Res*, 42 (3) (2017) 318.
- 8 Gedilu M, Santhanam S, Bogale M & Selvaraj S K, *J Eng Fibers Fabr*, 17 (2022) 1.
- 9 Sundaresan S, Sivanganam K J & Kumar A S, *Int J Eng Technol*, 8 (5) (2019) 712.
- 10 Pazireh E, Gharehaghaji A A & Haghighat E, *J Eng Fibers Fabr*, 9 (4) (2014) 83.
- 11 Q Chen, J Fan & C Sun, *Fibers Polym*, 16 (9) 2077 (2015).
- 12 Chidambaram P, Govindan R & Venkatraman K C, *AJBAS*, 4 (2) (2012) 60.
- 13 Oglakcioglu N, Celik P, Marmarali A, Ute T B, Marmarali A & Kadoglu H, *Text Res J*, 79 (10) (2009) 888.
- 14 Jhanji Y, Gupta D & Kothari V K, *Indian J Fibre Text Res*, 40 (1) (2015) 11.
- 15 Ozdil N, Marmarali A & Kretzschmar S D, *Int J Therm Sci*, 46 (12) (2007) 1318.
- 16 Yazdi M M, Semnani D & Sheikhzadeh M, *J Appl Polym Sci*, 114 (3) (2009) 1731.
- 17 Long H R, *Int J Cloth Sci*, 11 (4) (1999) 198.
- 18 Toma D, Popescu A, Niculescu C, Salistean A, Lite C, Neneciu M, Wechsler S, Ion ID, Puiu MG & Raigan C, *Ind Text*, 74(6) (2023) 753.
- 19 Sayed A, Khalil E, Akter H, Islam A, Miah S, Al M & Aman U, *Advanced Research Journal*, 12 (1) (2025) 16.
- 20 Hossain M A & Islam M R, *J Eng Fibers Fabr*, 19 (2024) 1.
- 21 Tabassum S, Najib I, Razzak Fera R, Islam S M, Hasan S M & Nahid-Ull-Islam M, *JARTE*, 6 (2) (2025) 1.
- 22 Padleckienė I, Stygienė L, Krauledas S, Abraitienė A & Sankauskaitė A, *Polym*, 17 (7) (2025) 903.
- 23 Dolanbay Dogan S & Kılinc N, *Fibers Polym*, 25 (3) (2024) 1137.
- 24 Limeneh D Y, Tesema A F, Rajan K, Abidi N & Yilma K T, *J Nat Fibers*, 21 (1) (2024) 2436054.
- 25 Bivainyte A & Mikucioniene D, *Fibres Text East Eur*, 19 (3) (2011) 69.
- 26 Oglakcioglu N & Marmarali A, *Textile and Apparel*, 20 (3) (2010) 213.
- 27 ASTM D3776, Standard test methods for mass per unit area (weight) of fabric, (2020).
- 28 ASTM D1777- 96, Standard Test Method for Thickness of Textile Materials (2019).
- 29 ASTM D737, Standard Test Method for Air Permeability of Textile Fabrics (2018).
- 30 BS 7209, British Standard Specification for Water Vapour Permeable Apparel fabrics (1990).
- 31 BS 4745, British Standard Test Method for Determination of thermal resistance of textiles (1990).
- 32 Spencer D J, *Knitting Technology A comprehensive handbook and practical guide: Technology & Engineering* (Woodhead Publishing, Cambridge) (2001) 99.
- 33 Bagherzadeh R, Gorji M, Latifi M, Payvandy P & Kong L X, *Fibers Polym*, 13 (4) (2012) 529.
- 34 Bagherzadeh R, Gorji M, Latifi M, Sheikhzadeh M & Sattari M, *Fibers Polym*, 8 (4) (2007) 386.
- 35 Kawabata S, *The standardisation and analysis of hand evaluation* (Textile Machinery Society of Japan) (1980).